

SIMULATION AND OPTIMIZATION OF THE SPOON-WHEEL TYPE MAIZE PRECISION SEED-METERING DEVICE BASED ON VIBRATION

勺轮式玉米精量排种器在振动条件下的仿真与优化

Qing WANG[#], Dandan HAN^{**}, Lin CHEN, Yuxia HUANG, Wei LI, Chao TANG¹

College of Mechanical & Electrical Engineering, Sichuan Agricultural University, Ya'an/China

Tel: 08352883018; E-mail: handd1988@126.com

Corresponding author: Dandan Han

DOI: <https://doi.org/10.35633/inmateh-73-37>

Keywords: maize; spoon-wheel type; seed-metering device; vibration; optimization; discrete element method

ABSTRACT

The DEM (discrete element method) simulation and optimization of the shapes and quantity of spoons of spoon-wheel disc in the spoon-wheel seed-metering device under vibrational conditions are investigated in this paper. EDEM (Engineering-DEM) software was adopted to establish DEM models of 'Zhongyu No.3' coated maize seeds and the spoon-wheel seed-metering device first, and four additional spoons of various shapes (labeled as K1~K5, respectively) were designed. The test results indicated that the acceleration of seeds in the Y-direction in spoons (K2~5) was all less fluctuating than those in the original spoon (K1), and the multiple rate was the largest in spoon (K5). The ultimate optimal working speed of the spoon-wheel maize precision planter in southwest China was identified as 3 km/h, with 22 spoons and the ideal spoon shape being K3. The bench validation test was executed under vibrational conditions based on the optimal spoon structure and operation settings. The qualified rate exceeded 94.5% at an operating speed of 3~4 km/h, while the multiple rate was less than 4%, the leakage rate was lower than 1.5%, and the variation coefficient was smaller than 25.5%. The variety adaptability test was launched when the working speed was 3 km/h. The qualified rates of various maize varieties were all more than 96.5%; the multiple and leakage rates were both less than 2%, which satisfied the technical requirements of maize precision sowing in southwest China. The qualified rates of various maize varieties were all more than 96.5%, and the multiple and leakage rates were both less than 2%, which satisfied the technical requirements of maize precision sowing in southwest China.

摘要

本文研究了振动条件下勺轮式排种器中排种盘勺轮的形状和数量的 DEM(离散元法)仿真和优化。首先采用 EDEM (工程-离散元法)软件建立了"仲玉 3 号"包衣玉米种子和勺轮式排种器的 DEM 模型, 并设计了 4 个不同形状的附加勺子(分别标记为 K1~K5)。试验结果表明, 勺子(K2~5)内种子在 Y 方向的加速度波动均小于原勺子(K1), 且勺子(K5)内种子加速度的重播指数最高。最终确定西南地区勺轮玉米精量播种机的最佳工作速度为 3 km/h, 勺子数量为 22 个, 理想勺子形状为 K3。根据最佳勺子结构和操作设置, 在振动条件下进行了台架验证试验。在工作速度为 3~4 km/h 时, 合格指数超过 94.5%, 重播指数小于 4%, 漏播指数小于 1.5%, 变异系数小于 25.5%。在工作速度为 3 km/h 时进行了品种适应性试验, 各玉米品种合格指数均在 96.5% 以上, 重播指数和漏播指数均小于 2%, 满足了西南地区玉米精量播种的技术要求。

INTRODUCTION

The operating environment of the planter in the field has an immediate impact on seeding efficacy (Yang et al., 2015; Liao et al., 2020). Since of the sticky soil and uneven terrain in southwest China, the planter will generate vibrations in the field due to the undulation of the ground, and the seed-metering device will also be vibrated up and down at the same time, which will lead to a decrease in sowing quality, as evidenced by an increase in leakage rate and poor plant distribution uniformity (Jiang et al., 2011; Boydas et al., 2007). Consequently, the influential issue of vibration on the seeding performance of planters has gradually attracted widespread attention from scholars at home and abroad (Joseph et al., 2004; Moore., 1991; Zhao et al., 2010).

¹ Qing Wang, M.S. Stud. Agr.; Dandan Han, Lecturer. Ph.D. Eng.; Lin Chen, Prof. Ph.D. Eng.; Yuxia Huang, M.S. Stud. Agr.; Chao Tang, M.S. Stud. Agr.; Wei Li M.S. Stud. Eng.

(#These authors contributed equally to this work and should be considered co-first authors.)

A less uniform spacing of seeds discharged from the seed-metering device into the seed furrow can be triggered by field vibrations of the planter, as dictated by Yang et al. (Yang et al., 2016; Yang et al., 2016). It has been investigated that planter vibration could enormously interfere with the seeding process of the seed-metering device, thus diminishing the uniformity of plant distribution and impairing the planter's functionality (Emrah., 2021). Wang et al. conducted field vibration tests on the 2BMZ-2 no-till precision maize planter, and the effects of vibration loads on the performance of the seed-metering device and maize seed falling trajectory were analyzed, establishing the groundwork for improving the seeding performance of the finger clip seed-metering device (Wang et al., 2015). The mathematical models of the vibration systems of the spade punch maize precision planter and the 2BM-5 air-suction no-till planter were constructed to explore the planter's vibration properties in the field (Zhang et al., 2014; Zhang et al., 2009; Liu et al., 2016). To investigate the effects of various vibration frequency intervals and amplitudes on seeding performance, the vibration test results of the 2BFQ-6 precision combine seeder in the field were conducted as guidance by Liao et al, providing a reference basis for research on increasing beneficial vibration intervals in practice (Liao et al., 2022; Zheng et al., 2023). Once the effects of vibration on the seeding performance of the seed-metering device have been identified, the ultimate objective is to enhance performance by eliminating the vibration impact. Wu et al. elevated the target seeding rate of a rapeseed centralized seed-metering device at different vibration frequencies by adjusting the longitudinal distance (Wu et al., 2022). The study by Min Y.B. et al. aimed to investigate the optimum vibration condition of the seed hopper on the vacuum suction nozzle seeder for improving seeding performance (Min Y.B. et al., 2008). Turgut et al. study that the planting units operate at different amplitudes and frequencies depending on the soil conditions of the field and the amplitude and frequency of the vibration vary according to the planter characteristics such as the planter weight, tire type, and tire pressure, as well as the surface smoothness of the field, the ratio of stone and clod (Turgut N. et al., 1992). The laboratory tests and field trials confirmed the expediency of using the engineering sample of the planting machine equipped with the vibration-pneumatic planting device, according to research by Aksenov et al. (Aksenov A.G. et al., 2018). Vishnyakov A.A. et al studied the main factors influencing the quality of seeding by vibration device are determined and according to research results, a graph of their influence on estimates of seeding was constructed (Vishnyakov A.A. et al., 2015).

Seed-metering device is the centerpiece of the planter (Huang et al., 2022; Bai et al., 2022; Su et al., 2022). Depending on how it operates, the seed-metering device can be classified as mechanical or pneumatic (Han et al., 2018; Shi et al., 2019; Gao et al., 2023). The spoon-wheel seed-metering device is a kind of mechanical that primarily relies on gravity to achieve seed-cleaning and seed-voting, which has the advantages of being less susceptible to damage, better sowing quality, and the ability to adapt to seeds with significant shape variations, among other things (Guo et al., 2019; Zhang et al., 2023), and it is the most widely used in production practice in southwest China. To identify the mechanism by which vibrations cause the seed-metering device to miss-sowing, the forces on the seeds during the seed-filling and seed-cleaning processes of the spoon-wheel seed-metering device are examined in this work. The major components of the seed-metering device are simulated and optimized to discover the ideal structure, which is subsequently verified in bench tests to reduce miss-sowing and increase spacing uniformity under vibration.

MATERIALS AND METHODS

Design of the spoon-wheel seed-metering device

Structure and working principle of the seed-metering device

The seed-metering device is the core component of the planter, and its structural parameters directly determine the sowing quality. The spoon-wheel seed-metering device, which is more typically adopted on planters in southwest China, consists of a rear shell, seed-guiding wheel, spacer plate, spoon-wheel disc, front shell, and other parts. The concrete structure of the seed-metering device is depicted in Fig. 1(a).

The seed-metering device is mainly fixed to and supported by the rear shell. The seeds are ladled up by the spoon on the spoon-wheel disc and delivered to the seed-guiding wheel. The initial position of the seed delivery from the spoon to the seed-guiding wheel is dictated by the opening location of the spacer plate, which separates the spoon-wheel disc from the seed-guiding wheel. The seed-guiding wheel receives the seed from the spoon-wheel disc and neatly releases it from the seed-metering device. The movement of seeds in the seed-metering device will be easily observed via the transparent front shell.

Everything that happens with the spoon-wheel seed-metering device can be divided into seed-filling, seed-cleaning, seed-delivery, seed-protection, and seed-voting, as illustrated in Fig. 1(b).

The seeds are fed into the seed-filling zone via the seeds-inlet, the spoon-wheel disc, and the seed-guiding wheel together rotate in tandem with the seeding shaft. The seeds are loaded into the spoon hole under the combined action of gravity and the stirring of the spoon-wheel disc and then arrive at the opening position of the spacer plate via the seed-cleaning zone with the rotation of the spoon-wheel disc. After entering the seed-delivery zone, the single seed will disengage from the seed-metering device in the seed-voting zone under the joint action of gravity and centrifugal force and fall into the corresponding groove of the seed-guiding wheel from the opening position of the spacer plate, completing the entire seeding process.

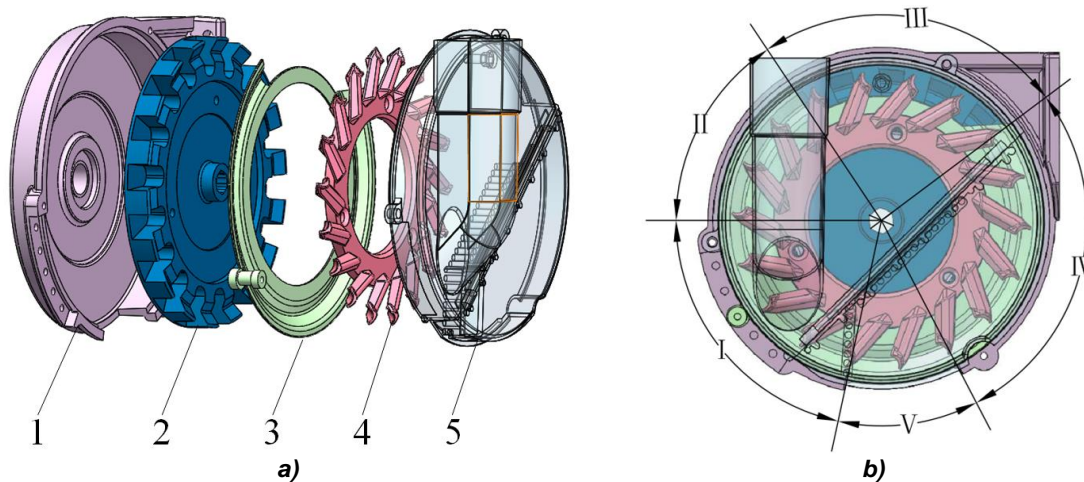


Fig. 1 - Schematic diagram of the spoon-wheel seed-metering device

a) Spoon-wheel seed-metering device; b) Diagram of the working process

1. Rear shell; 2. Seed-guiding wheel; 3. Spacer plate; 4. Spoon-wheel disc; 5. Front shell;

I. Seed-filling zone; II. Seed-cleaning zone; III. Seed-delivery zone; IV. Seed-protecting zone; V. Seed-voting zone

Force analysis of the seed-filling process

A good seed-filling effect is required for the seeding performance of the spoon-wheel seed-metering device (Pareek et al., 2021). The seed-metering device is driven by the ground wheel when the planter is running in the field. The seeds in the seed-filling zone are disturbed by the stirring action of the spoon-wheel disc, and the seeds near the spoon will follow the disc in a circular motion, thus fulfilling the seed-filling process. Planters may be subject to vibration during field operations due to the sticky soil and uneven terrain in southwest China. The seed-metering device will also be vibrated up and down with the planter. The forces on the seed during the seed-filling process are displayed in Fig. 2. The vibrating force on the seed-metering device is simplified to a vertical force in this paper.

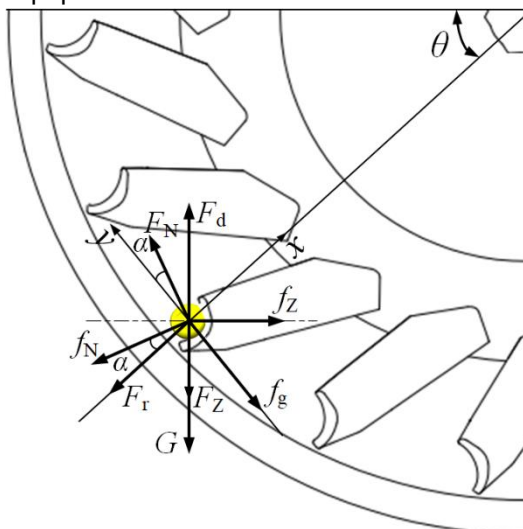


Fig. 2 - Force analysis diagram of the seed-filling process

The following equations can be derived from the analytical depiction of the forces on the seeds during the seed-filling process shown in Fig. 2.

$$F_r = mr\omega^2 \tag{1}$$

$$G = mg \tag{2}$$

$$f_N = F_N \tan \beta_1 \tag{3}$$

$$f_z = F_z \tan \beta_2 \tag{4}$$

$$f_g = F_g \tan \beta_3 \tag{5}$$

Where:

F_r is the centrifugal force generated by the seed's rotation with the spoon-wheel disc in N, G is gravity of seed in N, f_N is the frictional force between the inner spoon wall and the seed in N, f_z is the inter-population frictional force in N, f_g is the frictional force between the spacer plate and the seed in N, m is the seed mass in kg, r is the distance between the seed centroid and the center of the spoon-wheel disc in m, ω is the angular velocity of the seed in rad/s, g is the gravitational acceleration in m/s², F_N is the supporting force exerted on the seed by the inner spoon wall in N, F_z is the extrusion force produced by the seed population in N, β_1 is the friction angle between the seed and the spoon in (°), β_2 is the friction angle between the seed and the spacer plate in (°), β_3 is the friction angle between the seeds in (°).

The seed will be securely placed in the spoon after the seed-filling process is done. The resultant force of the forces acting on the seed in the x-axis direction is 0. The supporting force (F_N) exerted on the seed by the inner spoon wall is collated as follows:

$$F_N = \frac{F_z \sin \theta + G \cos \theta + f_N \cos \theta + F_r - f_z \cos \theta - F_d \sin \theta}{\sin \alpha} \tag{6}$$

where: F_d is the vertical vibrating force exerted on the seed by the seed-metering device vibrating in the field with the planter in N, α is the inclination angle of the spoon (°); and θ is the angle between the spoon and the center of the spoon-wheel disc (°).

As can be observed from Eq. (6), the supporting force (F_N) applied to the seed by the inner spoon wall diminishes as the vertical vibrating force (F_d) exerted on the seed by the vibration of the seed-metering device increases. Thus, the supporting force on the seed by the inner spoon wall is needed to be greater than 0 ($F_N > 0$) for the seed inside the spoon to remain in place. Otherwise, the supporting force (F_N) exerted on the seed by the inner spoon wall will be zero when the vertical vibrating force (F_d) surpasses a particular value, resulting in seed-filling failure and missed sowing.

Force analysis of the seed-cleaning process

When there are multiple seeds in the spoon, the seeds located on the outside of the spoon will gradually detach from the spoon and fall back into the seed-filling zone again under the combined force of gravity and other external forces, leaving only one seed in the spoon, which is referred to as the “seed-cleaning process” of the spoon-wheel seed-metering device. In this case, the single seed inside the spoon is exposed to gravity (G), the supporting force (F_N) exerted on the seed by the inner spoon wall, the frictional force (f_N) between the inner spoon wall and the seed, the centrifugal force (F_r) generated by the rotation of the seed with the spoon-wheel disc, the frictional force (f_g) between the spacer plate and the seed, and the vertical vibrating force (F_d) caused by the vibration of the seed-metering device. The forces acting on the seed during the seed-cleaning process are illustrated in Fig. 3.

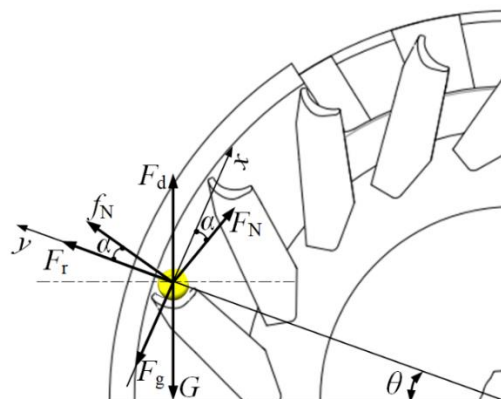


Fig. 3 - Force analysis diagram of the seed-cleaning process

The resultant force of the projected forces on the seed in the x-axis is:

$$F_x = f_N \sin \alpha + F_N \cos \alpha + F_d \cos \theta - G \cos \theta - f_g \tag{7}$$

Smooth seed cleaning can only be achieved during the seed-cleaning process if the resultant force of the projected forces in the x-axis on the seed is greater than zero. In this instance, the supporting force (F_N) on the seed by the inner spoon wall satisfies the following relationship:

$$F_N > \frac{G \cos \theta + f_g - f_N \sin \alpha - F_d \cos \theta}{\cos \alpha} \tag{8}$$

When the seed-metering device vibrates vigorously in the field with the planter, an increase in the vertical vibrating force (F_d) exerted on the seed by the vibration of the seed-metering device will result in a reduction in the supporting force (F_N) provided by the inner spoon wall. The seed-cleaning function of the seed-metering device is unaffected unless the vibrating force (F_d) is within a specific range. Consequently, if the seed-metering device vibrates excessively when the planter is in the field, it will lead to excessive seed-cleaning, which will trigger all of the seeds in the spoon to be shaken back into the seed-filling zone, resulting in an airlift of the seed spoon and unsuccessful sowing.

Planters will inevitably vibrate when operating in the field due to the sticky soil and uneven terrain in southwest China. Hence, it is required to optimize the structure of the existing spoon-wheel seed-metering device to make it more adaptable to the working circumstances in southwest China.

Optimized design of the spoon-wheel seed-metering device

Structural optimization of the spoon

The spoon-wheel disc is the core component of the spoon-wheel seed-metering device, and the spoon of the spoon-wheel disc is the primary working portion for taking and carrying seeds. The seed-filling, seed-cleaning, and seed-delivery effects of the seed-metering device are influenced by the spoon's shape (Jia et al., 2018). According to the above-mentioned forces on the seed during the seed-filling and seed-cleaning process, as well as the spoon design requirements, this paper is devoted to optimizing the spoon structure to lower the leakage rate caused by vibrations during the seed-metering device's function in the field.

The spoon employed in the existing spoon-wheel seed-metering device is based on a tetrahedral construction with a cylinder at an angle in particular through, eliminating the part where they are intersected, and the spoon hole is made on the curved surface formed on the tetrahedron (Jia et al., 2018). The specific structure of the spoon is illustrated in Fig. 4. The central axis of the cylinder is denoted by Y_1 , R_1 is the radius of the cylinder, and α_1 is the angle between the cylinder and the tetrahedron. To guarantee that the spoon can successfully scoop up more than one seed at a time, the spoon hole is required to be larger than the maximum length of the maize seed. Accordingly, the radius of the spoon hole and the size of the maize seed has the following relationship:

$$2R > L \tag{9}$$

R_{min} is the minimum radius of the cylinder in mm and L is the maximum length of the maize seed in mm.

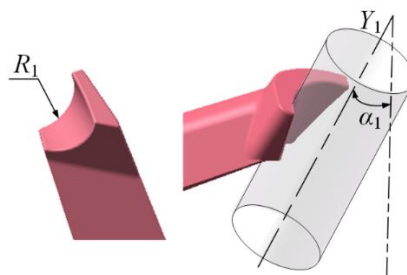


Fig. 4 - Schematic diagram of the shape of the original spoon hole

It can be observed that the vibration will mostly result in a reduction of the supporting force (F_N) on the seed by the inner spoon wall from the analysis of the forces on the seed during the seed-filling and seed-cleaning processes. To ameliorate the substantial leaping of the seeds triggered by vibrations that detach them from the spoon, the original spoon hole was twice incised with a cylinder of radius R_2 . In this instance, the angle formed by the axes of cylinder 2 (Y_2) and cylinder 1 (Y_1) is β . The optimal structure of the spoon nest can be acquired by eliminating the intersection between cylinder 2 and the original spoon nest. The structural layout of the sliced spoon nest is depicted in Fig. 5.

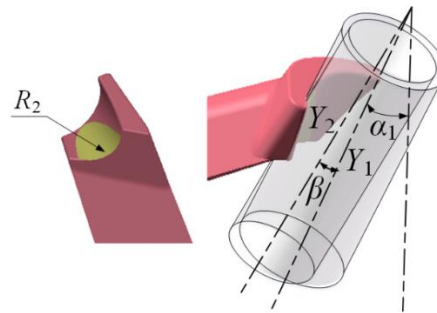


Fig. 5 - Schematic diagram of the improved spoon hole

Structural optimized design of the spoon

The maize variety that is commonly grown in southwest China is 'Zhongyu No. 3'. The measurement of the triaxial dimensions of maize seeds has been completed in the preliminary stage, and the results are listed in Table 1. The optimized spoon nest is based on the original structure for secondary cutting and shaping. The criterion " $R_2 < R_1$ " needs to be fulfilled to avoid interfering with the current seed-filling function of the spoon nest and disrupting the general shape of the original spoon nest. $2R_2$ should be longer than the average length of the maize seeds to comply with the design requirements of the spoon nest. As indicated in Table 1, the average length of maize seeds was 10.92 mm, and R_2 was determined to be 5.5 mm in this paper.

Table 1

| Triaxial sizes of 'Zhongyu No. 3' maize seeds | | | |
|---|-------------|------------|-------------|
| Seeds | Length [mm] | Width [mm] | Height [mm] |
| Flat | 10.92 | 8.31 | 4.96 |
| Spherical | 8.90 | 8.43 | 7.15 |

Analyzing the forces acting on the seed throughout the seed-filling and seed-cleaning processes reveals that the inclination angle (β) between the cylinder and the tetrahedron is essential for guaranteeing the seeds to fill the spoon hole smoothly. The seed travels from the spoon into the groove of the seed-guiding wheel mainly relying on gravity when the seed-metering device is in use. The spoon was 3D modeled with SolidWorks (version 2022) at different angles (β). In particular, when β is greater than 10° , it will conflict with the contoured shape of the original spoon. Additionally, without altering the profile of the original spoon, the bigger the β , the larger the overall shape of the spoon will be, which will result in multiple seeds filling the spoon at one time, thus affecting the single rate of seeding. The original spoon was thereby designated K1, and K2, K3, K4, and K5 are the spoons that were designed for an β 1° , 3° , 5° , and 7° , respectively. The structures of various spoons are depicted in Fig. 6.

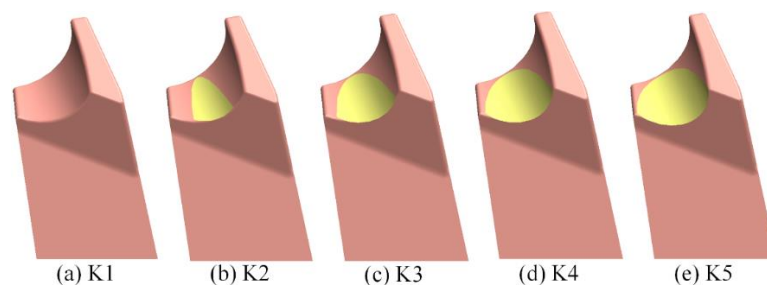


Fig. 6 - Different structures of spoon holes

Simulation and optimization DEM particle modelling

Maize seeds can be classified as "flat" and "spherical" according to the morphological characteristics of 'Zhongyu No. 3'. Statistically, there are around 74% flat maize seeds and roughly 26% spherical seeds. The coated maize seeds were virtually modeled in SolidWorks using their length, width, and height measurements from Table 1, and the 3D models were then imported into the EDEM software (version 2018) in '.step' format. The Multi-sphere method was executed to establish the DEM models of maize seeds, as shown in Fig. 7.

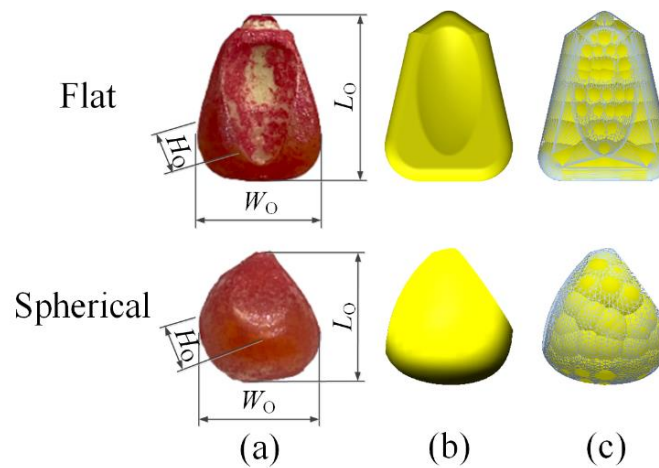


Fig. 7 - Models of maize seed
(a) Physical figure; (b) 3D model; (c) EDEM model

DEM modelling of the seed-metering device

The spoon-wheel type seed-metering device is essentially composed of the rear shell, seed-guiding wheel, spacer plate, spoon-wheel disc, and transparent front shell. To conserve simulation time, elements unrelated to seed movement, such as bearings and bolts, were omitted without compromising simulation results. The simplified 3D model of the seed-metering device built with SolidWorks was loaded into the EDEM's pre-processing module in '.step' format. Aluminum alloy was adopted as the basic material for the spoon wheel discs. The DEM characteristics of the 'Zhongyu No. 3' coated maize seeds have been measured and calibrated in advance (Han *et al.*, 2023). The contact parameters between the maize seeds and the seed-metering device are listed in Table 2.

Table 2

| Simulation input parameters of maize and seed-metering device | | |
|---|-------|----------------------|
| Parameters | Maize | Seed-metering device |
| Poisson's ratio | 0.398 | 0.250 |
| Shear modulus [MPa] | 177 | 27000 |
| Density [g/cm ³] | 1.094 | 2.700 |
| Restitution coefficient [with maize] | 0.380 | 0.675 |
| Static friction coefficient [with maize] | 0.237 | 0.444 |
| Rolling friction coefficient [with maize] | 0.029 | 0.103 |

A virtual particle factory is followed by building above the inlet of seeds once the simulation parameters have been set. The movability of the spoon-wheel disc and seed-guiding wheel were arranged to be linear rotation, and the rotating speed of each group during the simulation was equal to the working speed of the planter. For all of the components were subjected to vertical vibration to simulate how the seed-metering device would operate under vibrational conditions, and the specific vibration parameters are indicated in Table 3.

A total of about 1500 particles were generated by the virtual factory based on the number of seeds in the chamber during the actual operation of the seed-metering device. Wherein 26% were spherical seeds and 74% were flat seeds.

The rotating time of the spoon-wheel disc and the seed-guiding wheel, as well as the vertical movement time of the seed-metering device, were started from 0.5 s when the particle generation in the chamber was complete and in a stable state. To extract motion information of particles in EDEM as precisely as feasible, the EDEM time step was set to 1×10^{-5} s, and data was recorded every 0.01 s.

The simulated working process of the spoon-wheel seed-metering device is illustrated in Fig. 8.

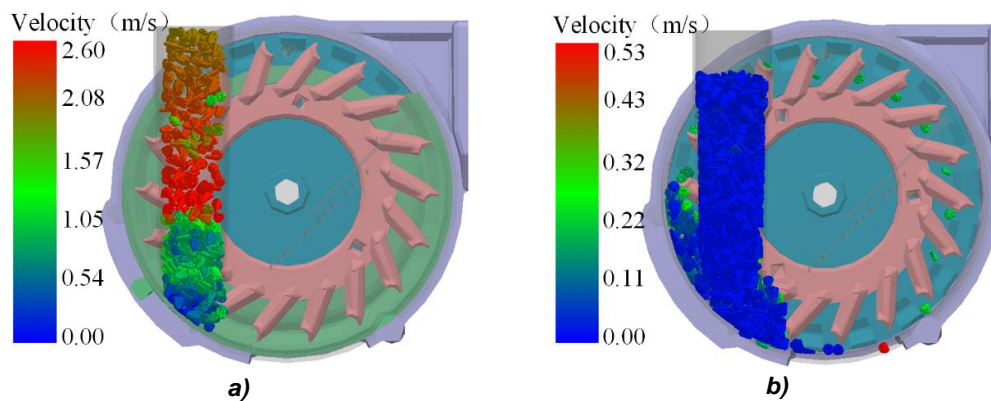


Fig. 8 - The working simulation process of the seed-metering device
a) Particle generating process; b) Seed arranging process

The different seeding phases of the spoon-wheel seed-metering device during the working process are depicted in Fig. 9.

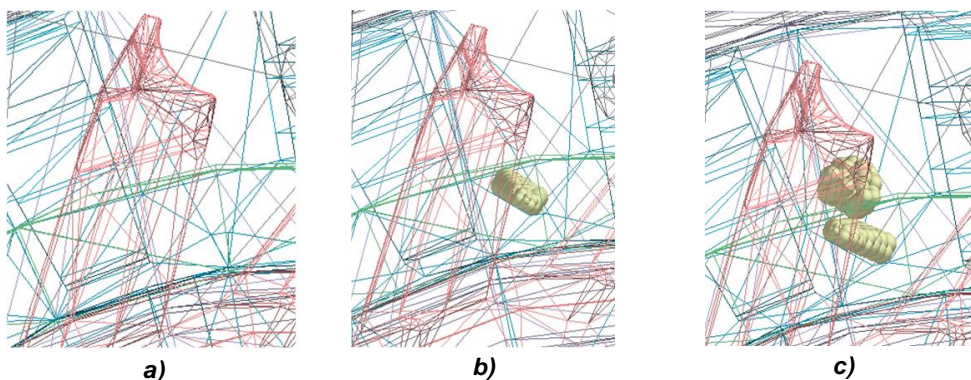


Fig. 9 - The seeding statuses of the seed-metering device
a) Leakage sowing state; b) Qualified sowing state; c) Multiple sowing state

Simulation of the spoon-wheel disc

Experimental design

The spoon quantity and the disc's diameter are the essential structural parameters of the spoon-wheel seed-metering device. The seed-metering device's overall constructional dimensions are determined by the diameter of the spoon-wheel disc, while its speed is dictated by the spoon quantity used. In this regard, the working speed of the planter and the linear velocity at the spoon of the spoon-wheel disc are correlated as displayed in (Ding *et al.*, 2018):

$$\frac{v_1}{v_2} = \frac{Zk}{2\pi R} \quad (10)$$

Where v_1 is the working speed of the planter in m/s; v_2 is the linear speed at the spoon of the spoon-wheel disc in m/s; R is the radius of the spoon-wheel disc in mm; Z is the number of the spoons; k is the theoretical plant spacing in mm.

At the same planter working speed and equivalent theoretical plant spacing, an increase in the number of spoons could reduce the rotation velocity of the spoon-wheel disc and thus improve the seeding performance. To investigate the influence of spoon-wheel discs with various numbers of spoons on the seeding performance under vibrational conditions, the optimization of the number of spoons was focused on in this section. The angle between two spoons on the spoon-wheel disc is φ_1 , with the spoon quantity (Z) and angle (φ_1) having the following relationship:

$$\varphi_1 = \frac{360^\circ}{Z} \quad (11)$$

The spoon mounted on the spoon-wheel disc is required to match the groove of the seed-guiding wheel, and the two components are synchronized with the seeding shaft. Consequently, the spoon-wheel disc and seed-guiding wheel need to be designed in compliance with the following condition: $\varphi_1 = \varphi_2$. The structure of the spoon-wheel disc and seed-guiding wheel are schematically diagrammed in Fig. 10.

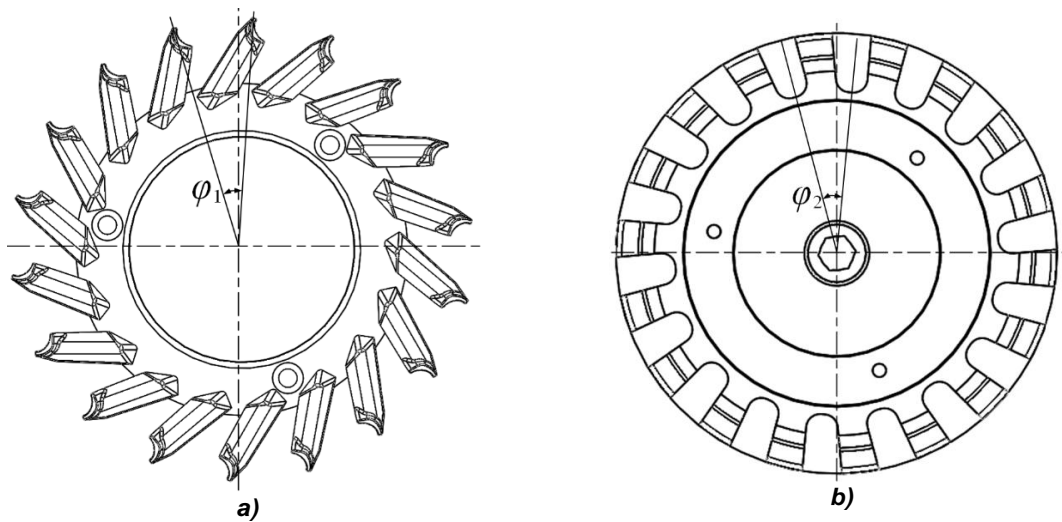


Fig. 10 - Schematic diagrams of the structure of spoon-wheel disc and seed-guiding wheel
 a) Spacing angle of the dipper wheel; b) spacing angle of the guide wheel

As noticed from Eq. (11), the angle between two spoons (φ_1) will decrease as the number of spoons (Z) extends while the diameter of the spoon-wheel disc remains constant. Currently, the most common quantity of spoons used in spoon-wheel devices is 18. Without altering the diameter of the spoon-wheel disc, up to 24 spoons can be manufactured. The number of spoons for comparative tests was selected at 18, 20, 22, and 24. Furthermore, it should be noted that the spoons of K2-4 are relatively neatly ordered as a result of the previously compared simulations of spoon-wheel discs with various spoon shapes. Therefore, the original spoon shape K1 and K2-4 were chosen for the comparative trials. A comparative test was carried out with the planter working at a speed of 3 to 6 km/h since the planter is less efficient while operating at a forward speed of 2 km/h in the field.

To obtain the optimal working parameters combination of the seed-metering device, the three factors-four levels orthogonal test was conducted in this part with the working speed, number of spoons, and structures of spoon holes as test factors, and the qualified rate, multiple rate, leakage rate, and variation coefficient of seeding as evaluation indicators. The orthogonal table $L^{16}(4^5)$ was selected, and the test factors and levels are listed in Table 3. The theoretical plant spacing was fixed at 20 cm in each trial group according to the agronomic requirements of maize cultivation in southwest China.

Table 3

| Factors and levels of the orthogonal test | | | |
|---|------------------------|--------------------|----------------------------|
| Levels | Factors | | |
| | A Working speed [km/h] | B Number of spoons | C Structure of spoon holes |
| 1 | 3 | 18 | K1 |
| 2 | 4 | 20 | K2 |
| 3 | 5 | 22 | K3 |
| 4 | 6 | 24 | K4 |

To simulate the field operation of the planter as well as for the measurement and statistics of each evaluation indicator, a 20 m-long seed bed was created under the seed-metering device to imitate the linear motion of the planter pulled by the tractor. The material properties of the seedbed and the variables governing the interaction between the seed and the seedbed were referred to in the earlier study findings (Lei et al., 2020; Wang et al., 2023). The specific parameter settings are shown in Table 4.

Table 4

| Simulation parameters setting of rubber and maize | | | | | | |
|---|-----------------|---------------------|------------------------------|--------------------------------------|--|---|
| Parameters | Poisson's ratio | Shear modulus [MPa] | Density [g/cm ³] | Restitution coefficient [with maize] | Static friction coefficient [with maize] | Rolling friction coefficient [with maize] |
| Rubber | 0.47 | 2900 | 1.350 | 0.0001 | 10 | 10 |

Note: To avoid seeds bouncing, the mechanical parameters of contact between maize and rubber are not true values.

The material properties of the seedbed and the variables governing the interaction between the seed and the seedbed were referred to in the earlier study findings (Lei *et al.*, 2020; Wang *et al.*, 2023). The specific parameter settings are shown in Table 4.

RESULTS

Simulation test results and analysis of the spoon hole

The analysis of the forces on the seed throughout the seed-filling and seed-cleaning processes revealed that the primary cause of the leaking of seeds was the seeds detached from the spoon holes. The original spoon hole (K1) was pre-simulated under vibrational conditions to better investigate the cause of the seeds falling back to the seed-filling zone in the event of vibration. The front shell is displayed as "Filled" in EDEM so that the phenomenon of leakage inside the seed-metering device can be observed. The opacity of the front shell is set to 0.1, while the spoon-wheel disc is set to 1. Following the observation of several seed-dropping procedures, it emerged that the seeds were most likely to detach from the spoon hole in the Y-direction during the seed-cleaning stage under vibrational conditions.

The phenomenon of leaking of the spoon-wheel seed-metering device under vibrational and the dropping direction of the seed is illustrated in Fig.11.

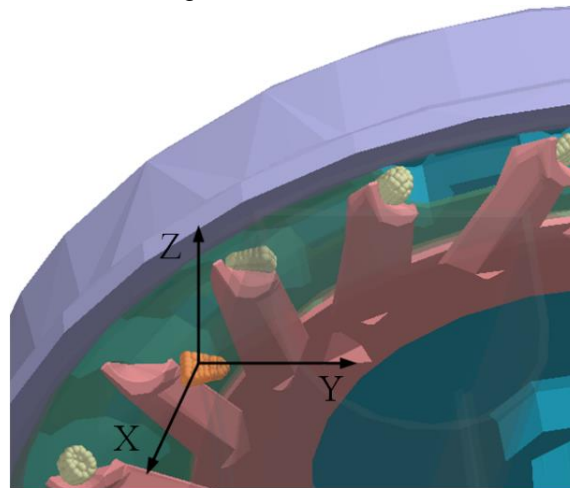


Fig. 11 - The dropping direction of maize seed

To optimize the seeding performance of the seed-metering device under vibrational conditions, comparative vibration tests were conducted for the spoon-wheel type planter at different working speeds. The vibration testing trials and analysis of the spoon-wheel planter in the field were performed in the foregoing period. DEM simulation tests were conducted on the aforementioned spoon-wheel discs with varied spoon holes under vibrational conditions for the spoon-wheel seed-metering device. In contrast, to analyze the stability of seeds moving in the Y-direction inside the spoon, three seeds with successful seed delivery were chosen at random after each group of simulations was completed.

The velocities of the selected seeds in the Y-direction inside the spoon during the seed-cleaning stage were exported, and the averaged values of their velocities were fitted by a MATLAB program to obtain the acceleration curves of the seeds concerning time.

The maximum difference between the acceleration of the seed and the spoon itself in the Y-direction for various spoon hole structures was calculated and gained by using the acceleration curve of the spoon itself as a baseline. Due to the considerable variation of the initial acceleration when the seed enters the spoon and the acceleration just before it is going to be released from the spoon and delivered to the seed-guiding wheel, the accelerations at these two limiting positions cannot be compared.

Comparisons of the Y-directional acceleration of seeds from the five kinds of spoon holes are illustrated in Figs. 12~16, respectively.

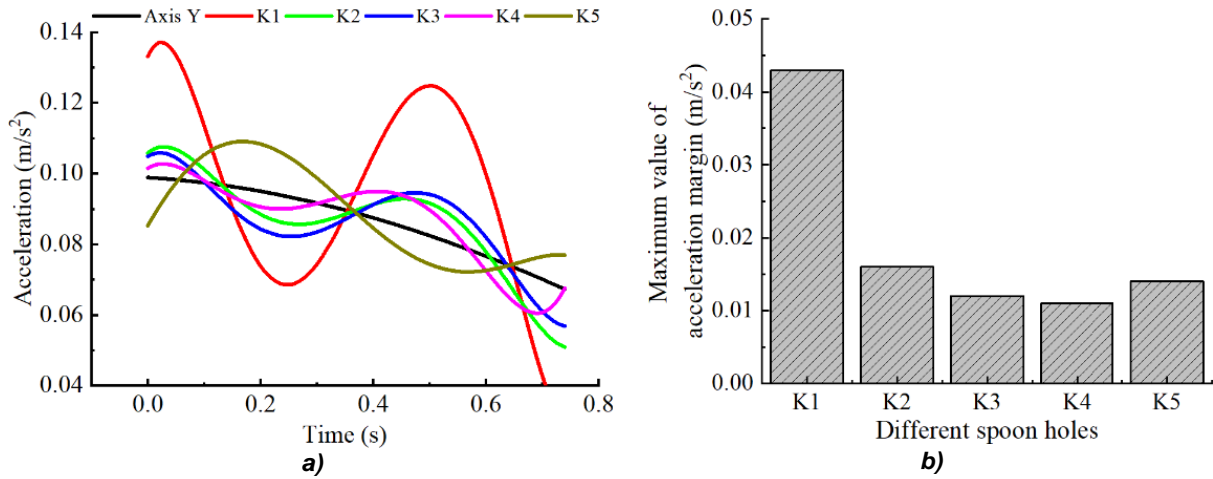


Fig. 12 - Comparative diagram of seed acceleration in the y-direction at a working speed of 2 km/h
 a) Acceleration change curve; b) Maximum difference of acceleration

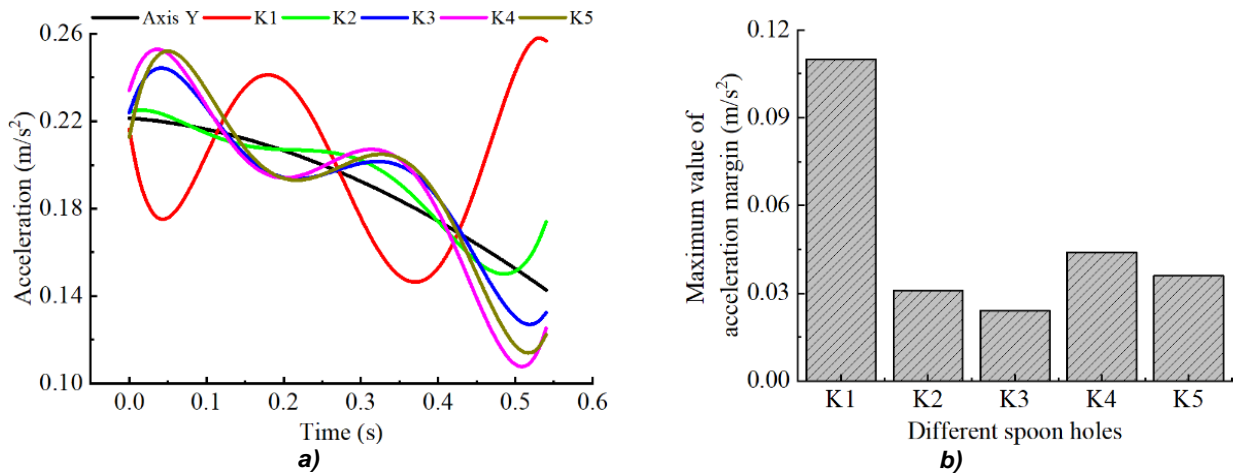


Fig. 13 - Comparative diagram of seed acceleration in the y-direction at a working speed of 3 km/h
 a) Acceleration change curve; b) Maximum difference of acceleration

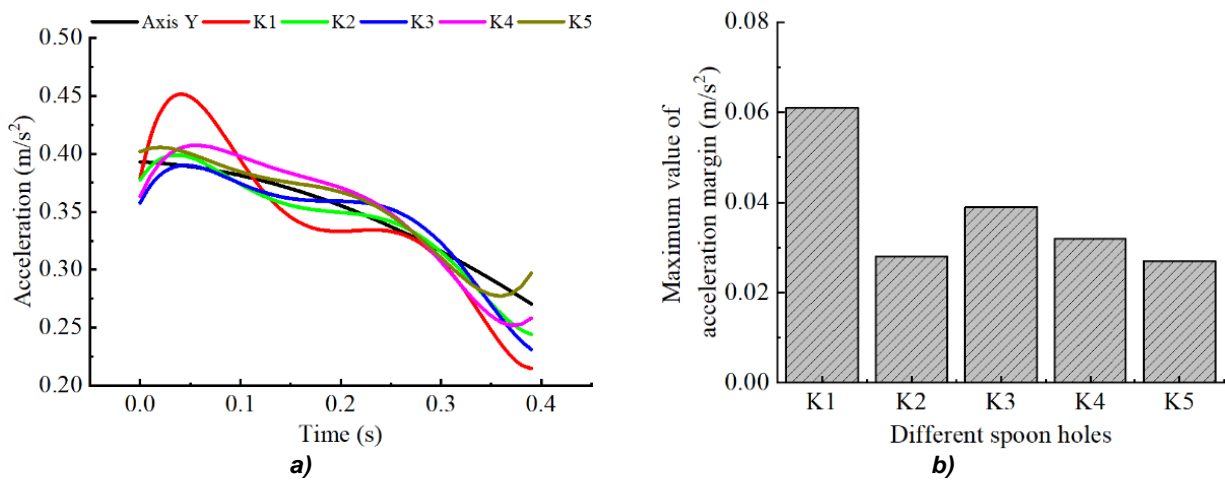


Fig. 14 - Comparative diagram of seed acceleration in the y-direction at a working speed of 4 km/h
 a) Acceleration change curve; b) Maximum difference of acceleration

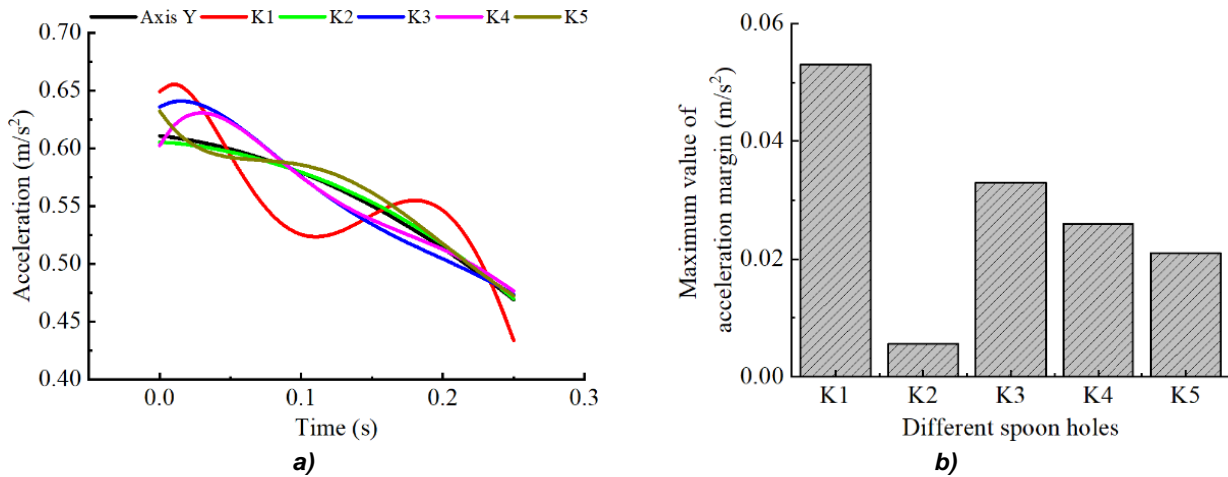


Fig. 15 - Comparative diagram of seed acceleration in the y-direction at a working speed of 5 km/h
 a) Acceleration change curve; b) Maximum difference of acceleration

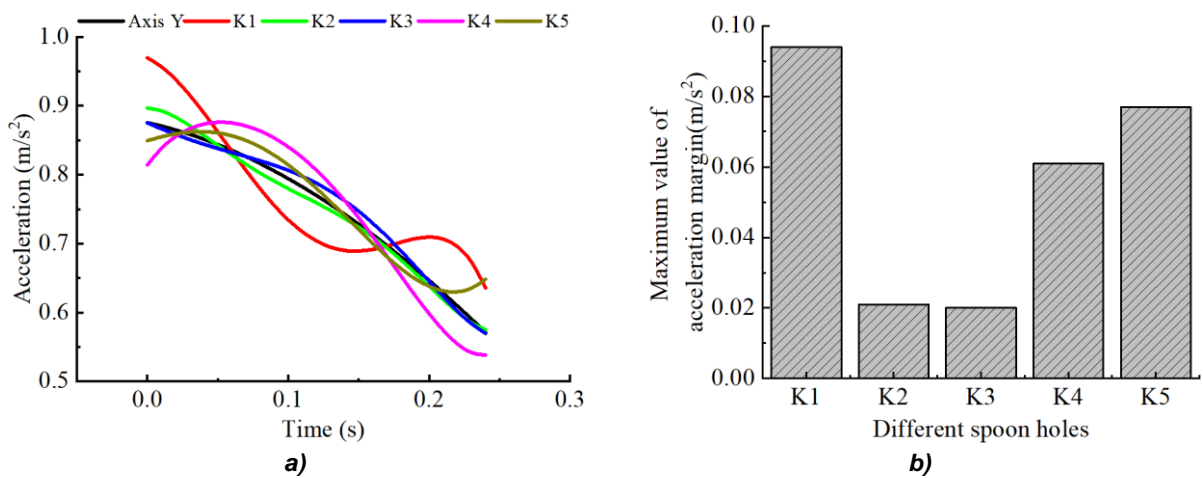


Fig. 16 - Comparative diagram of seed acceleration in the y-direction at a working speed of 6 km/h
 a) Acceleration change curve; b) Maximum difference of acceleration

It was revealed that the acceleration in the Y-direction of seeds in spoons K2-5 was less fluctuating than those in spoon K1 when the working speed was 2-6 km/h by analyzing the variation in an acceleration of maize seeds at a variety of working speeds and within diverse spoon structures, which indicates that the seeds would be more stable in these four spoons of K2-5. The anomalous states of the seeds being fed from the spoon-wheel disc into the seed-guiding wheel in the DEM simulation are reseeding (2 or more seeds in the seed-guiding wheel) and missing (0 seeds in the seed-guiding wheel). In addition to comparing the stability of seeds moving in the Y-direction, it is required to evaluate the aberrant states of seeds entering the seed-guiding wheel from the spoon-wheel disc within the five species of spoons. The results are shown in Fig. 17.

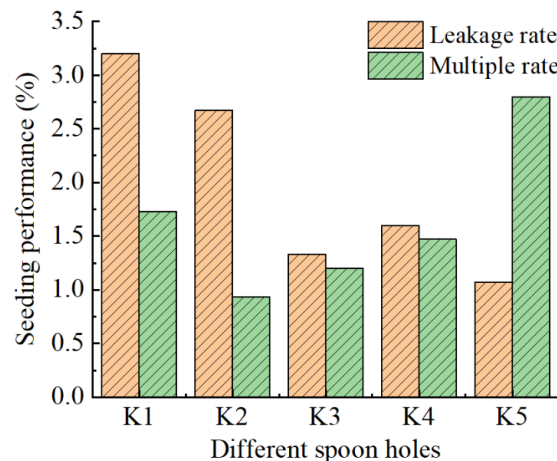


Fig. 17 - Comparison of the seeding performance of various spoon-wheel discs

According to Fig. 16, the leakage rate of all four species of spoons (K2~5) is lower than the rate of the original spoon (K1), while the multiple rate of spoon (K5) is the highest. Therefore, the seeding performance of spoons (K2~4) is relatively more stable.

Simulation of the spoon-wheel disc experimental results and analysis

Each set of DEM simulation tests was repeated thrice, and the distance between seeds was measured using the post-processing tool “ruler” in EDEM, as indicated in Fig. 18.

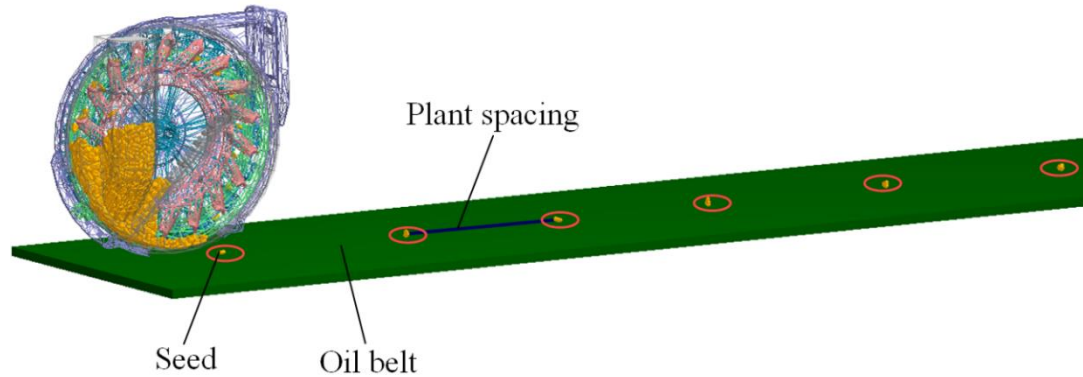


Fig. 18 - Simulation result of the seed-metering device on the oil belt

The design scheme and results of the orthogonal test are listed in Table 5.

Table 5

| Simulation results of the orthogonal test | | | | | | | |
|---|---|---|---|--------------------|-------------------|------------------|---------------------------|
| No. | A | B | C | Qualified rate [%] | Multiple rate [%] | Leakage rate [%] | Variation coefficient [%] |
| 1 | 1 | 1 | 1 | 96.15 | 1.13 | 2.72 | 20.73 |
| 2 | 1 | 2 | 2 | 97.25 | 0.05 | 2.70 | 20.55 |
| 3 | 1 | 3 | 3 | 97.45 | 1.14 | 1.41 | 17.10 |
| 4 | 1 | 4 | 4 | 97.01 | 1.30 | 1.69 | 22.74 |
| 5 | 2 | 1 | 2 | 94.59 | 2.13 | 3.28 | 27.82 |
| 6 | 2 | 2 | 1 | 93.36 | 3.97 | 2.67 | 27.64 |
| 7 | 2 | 3 | 4 | 95.93 | 2.91 | 1.16 | 25.71 |
| 8 | 2 | 4 | 3 | 93.47 | 4.73 | 1.80 | 25.13 |
| 9 | 3 | 1 | 3 | 90.93 | 4.80 | 4.27 | 27.50 |
| 10 | 3 | 2 | 4 | 91.97 | 4.32 | 3.71 | 29.62 |
| 11 | 3 | 3 | 1 | 95.83 | 1.09 | 3.08 | 24.73 |
| 12 | 3 | 4 | 2 | 91.94 | 3.38 | 4.68 | 31.52 |
| 13 | 4 | 1 | 4 | 88.41 | 3.76 | 7.83 | 31.80 |
| 14 | 4 | 2 | 3 | 88.78 | 4.85 | 6.37 | 29.02 |
| 15 | 4 | 3 | 2 | 90.92 | 1.67 | 7.41 | 27.32 |
| 16 | 4 | 4 | 1 | 90.72 | 2.72 | 6.56 | 29.68 |

Analysis of variance (ANOVA) was executed to examine the findings of the orthogonal test, and the results are presented in Table 6.

Table 6

| Variance analysis of orthogonal test results | | | | | | | |
|--|--------------------|----------------|----|-------------|---------|---------|--------------|
| Dependent variable | Source of variance | Sum of squares | Df | Mean square | F-value | P-value | Significance |
| Qualified rate | A | 111.031 | 3 | 37.010 | 42.118 | 0.000 | ** |
| | B | 15.059 | 3 | 5.020 | 5.712 | 0.034 | * |
| | C | 4.034 | 3 | 1.345 | 1.530 | 0.300 | - |

| Dependent variable | Source of variance | Sum of squares | Df | Mean square | F-value | P-value | Significance |
|-----------------------|--------------------|----------------|----|-------------|---------|---------|--------------|
| Multiple rate | Error | 5.272 | 6 | 0.879 | | | |
| | A | 18.170 | 3 | 6.057 | 14.948 | 0.003 | ** |
| | B | 6.075 | 3 | 2.025 | 4.998 | 0.045 | * |
| | C | 10.169 | 3 | 3.390 | 8.365 | 0.015 | * |
| Leakage rate | Error | 2.431 | 6 | 0.405 | | | |
| | A | 63.157 | 3 | 21.052 | 135.507 | 0.000 | ** |
| | B | 3.300 | 3 | 1.100 | 7.080 | 0.021 | * |
| | C | 2.668 | 3 | 0.889 | 5.724 | 0.034 | * |
| Variation coefficient | Error | 0.932 | 6 | 0.155 | | | |
| | A | 201.468 | 3 | 67.156 | 56.552 | 0.000 | ** |
| | B | 32.593 | 3 | 10.864 | 9.149 | 0.012 | * |
| | C | 18.027 | 3 | 6.009 | 5.060 | 0.044 | * |
| | Error | 5.145 | 6 | 0.858 | | | |

*Note: * means significant influence in 95% confidence interval, ** means significant influence in 99% confidence interval, - means no significant influence.

As observed in Table 6 of the ANOVA of the orthogonal test results, the effects of planter working speed (A) and spoon count (B) were both extremely significant and generally significant for all evaluation indicators, respectively. The spoon shape (C) had a typically considerable impact on the multiple rate, leakage rate, and variation coefficient, while it did not affect the qualified rate. It was discovered that the working speed of the planter extremely affects the seeding performance and that adding the number of spoons can improve seeding properties to some amount. While optimizing the shape of spoons will not enhance the qualified rate or the variation coefficient of plant spacing, it may somewhat ameliorate the multiple rate and leakage rate.

The orthogonal test results were evaluated for extreme differences, and the results are indicated in Table 7.

Table 7

Results of the extreme difference analysis

| Evaluation indicators | Factors | Levels | | | | Extreme Difference | Optimal level | Optimal combination |
|-----------------------|---------|--------|-------|-------|-------|--------------------|---------------|---------------------|
| | | k_1 | k_2 | k_3 | k_4 | | | |
| Qualified rate | A | 96.97 | 94.34 | 92.67 | 89.71 | 7.29 | 1 | |
| | B | 92.52 | 92.84 | 95.03 | 93.29 | 2.19 | 3 | $A_1B_3C_3$ |
| | C | 94.02 | 93.68 | 92.66 | 93.33 | 1.36 | 3 | |
| Multiple rate | A | 0.91 | 3.44 | 3.40 | 3.25 | 2.53 | 1 | |
| | B | 2.96 | 3.30 | 1.70 | 3.03 | 1.60 | 3 | $A_1C_2B_3$ |
| | C | 2.23 | 1.81 | 3.88 | 3.07 | 2.07 | 2 | |
| Leakage rate | A | 2.13 | 2.23 | 3.94 | 7.04 | 4.91 | 1 | |
| | B | 4.53 | 3.86 | 3.27 | 3.68 | 1.26 | 3 | $A_1B_3C_3$ |
| | C | 3.76 | 4.52 | 3.46 | 3.60 | 1.06 | 3 | |
| Variation coefficient | A | 20.28 | 26.58 | 28.34 | 29.46 | 8.06 | 1 | |
| | B | 26.96 | 26.71 | 23.72 | 27.27 | 3.25 | 3 | $A_1B_3C_3$ |
| | C | 25.70 | 26.80 | 24.69 | 27.47 | 2.78 | 3 | |

As revealed in Table 8 of the analysis of extreme differences in orthogonal test results, the primary and secondary factors affecting the qualified rate were $A>B>C$, and the optimal parameters combination was $A_1B_3C_3$. The major and secondary factors regarding the multiple rate were $A>C>B$, and the optimum set of combined factors was $A_1C_2B_3$. The principal and subsidiary factors that affected the leakage rate were $A>B>C$, and the ideal portfolio was $A_1B_3C_3$.

The priority factors influencing the coefficient of variation were $A > B > C$, and the optimized set was $A_1 B_3 C_3$. The results of the extreme difference analysis further indicated that the optimal levels of the planter working speed (A) and the number of spoons (B) were identical for each evaluation index, which were A_1 and B_3 , respectively. The preferred level of spoon shape (C) for the multiple rate was C_2 , while the intended level for the other three evaluation indicators was C_3 . Taking into account the fact that a slightly higher multiple rate throughout the sowing process would not detract from the overall working effectiveness of the planter. The integrated analysis ultimately concluded that the best working speed of the spoon-wheel maize precision planter is 3 km/h, the ideal number of spoons is 22, and the equivalent spoon shape is K3 under the conditions of sticky soil in southwest China.

Bench validation tests

Validation test of the spoon-wheel disc

The orthogonal test optimization results of DEM simulation ultimately led to the conclusion that 22 spoons and the shape of K3 contribute to the ideal structure of the spoon-wheel disc. A 3D model of the seed-guiding wheel with an identical number of grooves (22) was sketched, and the aluminum alloy material was adopted for 3D printing. Comparative bench tests of seeding performance at different working speeds were carried out for the optimized disc (S1), the original spoon-wheel disc (18 spoons, S2), and the commercially available spoon-wheel disc with 24 spoons (S3). The results are summarized in Table 8.

Table 8

| | Qualified rate [%] | | | Multiple rate [%] | | | Leakage rate [%] | | | Variation coefficient [%] | | |
|---|--------------------|-------|-------|-------------------|------|------|------------------|-------|------|---------------------------|-------|-------|
| | S1 | S2 | S3 | S1 | S2 | S3 | S1 | S2 | S3 | S1 | S2 | S3 |
| 3 | 97.45 | 94.33 | 94.67 | 1.14 | 1.34 | 1.67 | 1.41 | 4.33 | 3.66 | 20.28 | 25.63 | 25.17 |
| 4 | 94.70 | 92.00 | 93.33 | 3.82 | 4.03 | 3.67 | 1.48 | 3.97 | 3.00 | 25.42 | 27.02 | 28.05 |
| 5 | 93.38 | 90.26 | 91.00 | 2.95 | 3.85 | 4.27 | 3.67 | 5.89 | 4.73 | 26.11 | 31.43 | 30.94 |
| 6 | 90.05 | 87.33 | 89.74 | 3.26 | 2.00 | 4.12 | 6.69 | 10.67 | 6.14 | 28.17 | 32.09 | 31.18 |

As seen from Table 8, the qualified rate of the optimized spoon-wheel disc under vibrational conditions with different forward speeds can reach over 90%, which is higher than that of the original spoon-wheel disc (18 spoons) and the spoon-wheel disc (24 spoons) already available on the market. The multiple rates are all lower than 5%, the leakage rates are all smaller than 7%, and the variation coefficients are all less than 30%. The seeding performance is improved compared with that before optimization, and satisfies the design specifications.

Variety adaptability test

With a working speed of 3 km/h and a theoretical plant spacing of 20 cm, several species of seeds, including 'Zhengdan 958', 'Ziyu 46', 'Chuandan 99', 'Denghai 618', and 'Zhengda 999', were selected to investigate the variety adaptability of the optimized spoon-wheel disc. The averaged values were retrieved by replicating each group of tests thrice, and the results are indicated in Table 9.

Table 9

| Maize varieties | Qualified rate [%] | Multiple rate [%] | Leakage rate [%] | Variation coefficient [%] |
|-----------------|--------------------|-------------------|------------------|---------------------------|
| Zhengdan 958 | 96.97 | 1.63 | 1.40 | 21.50 |
| Ziyu 46 | 96.65 | 1.73 | 1.62 | 22.17 |
| Chuandan 99 | 97.30 | 1.53 | 1.17 | 21.53 |
| Denghai 618 | 97.07 | 1.26 | 1.67 | 21.42 |
| Zhengda 999 | 97.19 | 1.28 | 1.53 | 20.14 |

The results revealed that the optimized spoon-wheel disc had higher adaptation to maize seeds, with the qualified rate of all five maize varieties being greater than 96.5%, the multiple rate and leakage rate being both less than 2%.

CONCLUSIONS

Based on the actual demand for precision sowing of maize under vibrational conditions in the hilly areas of Southwest China, the key structure and working parameters affecting the precision sowing of the spoon-wheel seed-metering device under vibrational conditions was analyzed. The critical parameters related to the sowing performance of the planter was optimized and examined. The main conclusions are as follows:

(1) According to the analysis of forces on the seeds during the seed-filling and seed-cleaning processes under vibrational conditions, it was ascertained that the vertical vibrating force exerted on the seed by the vibration of the seed-metering device will induce a reduction in the supporting force on the seed by the inner spoon wall, which will increase the leakage rate of the seed-metering device under vibrational conditions. To address this issue, the simulated optimization and tests of the structures and number of spoons are carried out in this paper.

(2) To the characteristics of the forced seeds in the spoon under vibrational conditions, the spoon-wheel discs with varied spoon structures were designed, and DEM simulation compared tests was conducted with the acceleration variation of seeds in the Y-direction in the spoon as the evaluation index to analyze the stability of different spoon shapes on seeds during the seed-cleaning process. The superior spoon shape was ultimately defined as K2~4.

(3) The optimal spoon structure was further evaluated by conducting a three-factor and four-level orthogonal test with the working speed, the number and structure of the spoon as the test factors, and the qualified rate, multiple rate, leakage rate, and variation coefficient of plant spacing as the evaluation indexes, and the ultimate best spoon shape of the spoon-wheel disc was K3, and the number of spoons was 22.

(4) The optimized spoon-wheel disc to different maize varieties has a sowing qualified rate greater than 96.5%, multiple and leakage rates both less than 2%, which complies with national standard requirements, and has a good variety of adaptability, as indicated by the results of the variety adaptability test.

ACKNOWLEDGEMENT

This work was supported by the Natural Science Foundation of Sichuan Province (2022NSFSC0138), the Technological Innovation R&D Projects of Chengdu Science and Technology Bureau (2022YF0501141SN), and the Listing Project of Rural Revitalization Research Institute of Sichuan Tianfu District (XZY1-11).

REFERENCES

1. Aksenov A. G., Izmaylov A. lu., Dorokhov. A.S., Sibirev A.V. (2018). Onion bulbs orientation during aligned planting of seed-onion using vibration-pneumatic planting device. *INMATEH - Agricultural Engineering*. Vol.55, No.2, pp.63-77. Moscow /Russian.
2. Bai, W., Li, Y., Yu, H., Zhao, D., Li, X., Zhao, X. (2022). Design and simulation optimization of positive and negative pressure seed-metering device (正负压式精量排种器设计与仿真优化). *Journal of Hebei Agricultural University*, Vol.45, No.4, pp115-122. Baoding/China.
3. Boydas, M. G., Turgut, N. (2007). Effect of vibration, roller design, and seed rates on the seed flow evenness of a studded feed roller. *Applied Engineering in Agriculture*, Vol.23, No.4, pp. 413-418. Erzurum/Turkey.
4. Ding, L., Yang, L., Liu, S., Yan, B., He, X., Zhang, D. (2018). Design of air suction high speed precision maize seed metering device with assistant seed filling plate (辅助充种种盘玉米气吸式高速精量排种器设计). *Transactions of the Chinese Society of Agricultural Engineering*, Vol.34, No.22, pp.1-11. Beijing/China.
5. Emrah, K. (2021) Field-scale evaluation of parameters affecting planter vibration in single seed planting. *Measurement*, Vol.184. Igdır/Turkey.
6. Gao, X., Xie, G., Li, J., Shi G., Lai, Q., Huang, Y. (2023). Design and validation of a centrifugal variable-diameter pneumatic high-speed precision seed-metering device for maize. *Biosystems Engineering*, Vol.227, pp.161-181. Yangling/China.
7. Guo, X., Zhang, H., Wu, J., Chen, T. (2019) Simulation research on spoon type seed metering device of sunflower seed based on EDEM (基于 EDEM 的勺轮式葵花排种器离散元仿真研究). *Journal of Chinese Agricultural Mechanization*, Vol.40, No.2, pp.19-24. Kunming/China.

8. Han, D, Xu, Y., Huang, Y., He, B., Dai, J., Lv, X., Zhang, L. (2023). DEM parameters calibration and verification for coated maize particles. *Computational Particle Mechanics*, Vol.10, No.6, pp.1931-1941. Yaan/China.
9. Han, D., Zhang, D., Jing, H., Yang, L., Cui, T., Ding, Y., Wang, Z., Wang, Y., Zhang, T. (2018). DEM-CFD coupling simulation and optimization of an inside-filling air blowing maize precision seed-metering device. *Computers and Electronics in Agriculture*, Vol.150, pp.426-438. Beijing/China.
10. Huang, Y., Li, P., Dong, J., Chen, X., Zhang, S., Liu, Y. (2022). Design and experiment of side-mounted guided high speed precision seed metering device for soybean (大豆高速播种机侧置导引式精量排种器设计与试验). *Transactions of the Chinese Society for Agricultural Machinery*, Vol.53, No.10, pp.44-53. Yangling/China.
11. Jia, S., Wei, L., Chen, C., Qiao, H., Li, H. (2018). Structure design of spoon wheel planter and analysis of seeds force (勺轮式排种器结构设计与种子受力分析). *Journal of Jilin Institute of Chemical Technology*, Vol.35, No.9, pp.41-45. Jilin/China.
12. Jia, S., Wei, L., Zhang, Z., Hao, S., Liu, Y., Sun, Z. (2018). Design and simulation of spoon wheel type seed metering device based on discrete element theory (基于离散元理论的勺轮式排种器设计与仿真). *Research and Exploration in Laboratory*, Vol.37, No.12, pp.124-128. Jilin/China.
13. Jiang, X., Zheng, J., Chi, Z. (2011). Study of mechanized seeding machinery selection for single corn planting in hilly area's rape stubble (丘陵山地油菜茬玉米净作机械化播种机械选型研究). *Southwest China Journal of Agricultural Sciences*, Vol.24, No.4, pp.1261-1264. Chengdu/China.
14. Joseph, G. L., Mike, R. (2004). Corn response to within row plant spacing variation. *Agronomy Journal*, Vol.96, No.5, pp.1464-1468. Wisconsin/America.
15. Lei, X., Yang, W., Yang, L., Liu, L., Liao, Q., Ren, W. (2020). Design and experiment of seed hill-seeding centralized metering device for rapeseed (油菜精量穴播集中排种装置设计与试验). *Transactions of the Chinese Society for Agricultural Machinery*, Vol.51, No.2, pp.54-64. Yaan/China.
16. Liao, Y., Li, C., Liao, Q., Wang, L. (2020). Research progress of seed guiding technology and device of planter (播种机导种技术与装置研究进展分析). *Transactions of the Chinese Society for Agricultural Machinery*, Vol.51, No.12, pp.1-14. Wuhan/China.
17. Liao, Y., Qi, T., Liao, Q., Zeng, R., Li, C., Gao, L. (2022). Vibration characteristics of pneumatic combined precision rapeseed seeder and its effect on seeding performance (气力式油菜精量联合直播机振动特性及对排种性能影响). *Journal of Jilin University (Engineering and Technology Edition)*, Vol.52, No.5, pp.1184-1196. Wuhan/China.
18. Liu, Y., Liu, F, Zhao, M., Dong, S., Zhang, X. (2016). Analysis of vibration test and vibration theory of air-suction no-tillage planter (气吸式免耕播种机的振动测试与振动理论分析). *Journal of China Agricultural University*, Vol.21, No.10, pp.109-116. Huhehaote/China.
19. Min Y. B., Kim S. T., Kwon H. D., Moon S. W., Kang D. H. (2008). Effect of the seed hopper vibration on the seeding performance of the vacuum suction nozzle seeder. *Journal of Biosystems Engineering*, Vol.33, No.3, pp. 179-185. Gyeongsang/Korea.
20. Moore, S. H. (1991) Uniformity of plant spacing effect on soybean population parameters. *Crop Science*, Vol.31, No.4, pp.1049-1051. State of Louisiana/America.
21. Pareek, C., Tewari, V., Machavaram, R., Nare, B. (2021). Optimizing the seed-cell filling performance of an inclined plate seed metering device using integrated ANN-PSO approach. *Artificial Intelligence in Agriculture*, Vol.5, pp.1-12. Kharagpur/India.
22. Shi, L., Sun, B., Zhao, W., Yang, X., Xin, S., Wang, J. (2019). Optimization and test of performance parameters of elastic air suction type corn roller seed-metering device (弹性气吸嘴式玉米滚轮排种器排种性能参数优化与试验). *Transactions of the Chinese Society for Agricultural Machinery*, Vol.50, No.10, pp.88-95+207. Lanzhou/China.
23. Su, W., Chen, Z., Lai, Q., Jia, G., Lv, Q., Tian, B. (2022) Design and test of wheel-spoon type precision seed-metering device for Chinese herbal medicine pinellia ternate (轮勺式半夏精密排种器设计与试验). *Transactions of the Chinese Society for Agricultural Machinery*, Vol.53, No.9, pp.60-71. Kunming/China.
24. Turgut N., Ulger P., Ozsert I. (1992). The effect of vibration upon the longitudinal seed distribution for some delivery mechanisms, in: *Agricultural Mechanization 14th National Congress*, pp.112-124. Samsun/Turkey.

25. Vishnyakov A. A., Vishnyakov A. S., Klak A. I. (2015). Seeding of rapeseed by the use of vibration sowing device of a seeder. *Tractors and Agricultural Machinery*, Vol.82, No.10, pp.36-39. Krasnoyarsk/Russia.
26. Wang, B., Liao, Q., Wang, L., Shu, C., Cao, M., Du, W. (2023). Design and test of air-assisted seed-guiding device of precision hill-seeding centralized seed-metering device for sesame. *Agriculture* Vol.13, No.2, pp.393. Wuhan/China.
27. Wang, Q., Zhu, L., Li M., Huang, D., Jia, H., Zhuang, J. (2019). Vibration characteristics of corn no-tillage finger-type precision planter and its effect on seeding performance (指夹式玉米免耕精密播种机振动特性及对排种性能的影响). *Transactions of the Chinese Society of Agricultural Engineering*, Vol.35, No.9, pp.9-18. Changchun/China.
28. Wu, W., Chang, C., Li, T., Hu, H., Zhou, Z., Yang, W., Guo, J., Zhu, P., Li, J., Hu, J., Cheng, H., Tao, Y., Zhou, W., Deng, F., Chen, Y., Ren, W., Lei, X. (2022). Seed-filling characteristics of a centralized seed-metering device for rapeseed caused by vibration. *Agriculture*, Vol.12, NO.07, pp.965. Yaan/China.
29. Yang, L., Yan, B., Cui, T., Yu, Y., He, X., Liu, Q., Liang, Z., Yin, X., Zhang, D. (2016). Global overview of research progress and development of precision maize planters. *International Journal of Agricultural and Biological Engineering*, Vol.9, No.1, pp.9-26. Beijing/China.
30. Yang, L., Yan, B., Zhang, D., Zhang, T., Wang, Y., Cui, T. (2016). Research Progress on Precision Planting Technology of Maize (玉米精密播种技术研究进展). *Transactions of the Chinese Society for Agricultural Machinery*, Vol.47, No.11, pp.38-48. Beijing/China.
31. Yang, L., Zhang, R., Gao, N., Cui, T., Liu, Q., Zhang, D. (2015). Performance of no-till corn precision planter equipped with row cleaners. *International Journal of Agriculture and Biological Engineering*, Vol.8, No.5, pp.15-25. Beijing/China.
32. Zhang, R., Liu, H., Wei, G., Zhou, J., Shi, S., Li, H., He, T. (2023). Design and test of key components of scoop type precision sorghum seed metering device (勺式高粱精量排种器关键部件设计与试验). *Journal of Agricultural Mechanization Research*, Vol.45, No.12, pp.215-219. Jinan/China.
33. Zhang, X., Li, C., Li, J., Zou, M. (2014). Mathematic vibration model of spade punch planter of maize. Trans (铲式玉米精密播种机振动特性模型建立与试验). *Transactions of the Chinese Society for Agricultural Machinery*, Vol.45, No.2, pp.88-93. Changchun/China.
34. Zhang, X., Li, C., Tang, Q., Yang, Y., Ma, Y. (2009). Vibration properties of spade punch planter of maize (铲式玉米精密播种机振动特性试验). *Journal of Shenyang Agricultural University*, Vol.40, No.6, pp.732-735. Shenyang/China.
35. Zhao, Z., Li, Y., Chen, J., Xu, L. (2010). Numerical analysis and laboratory testing of seed spacing uniformity performance for vacuum-cylinder precision seeder. *Biosystems Engineering*, Vol.106, No.4, pp.344-351. Zhenjiang/China.
36. Zheng, J., Liao, Y., Qi, T., Liao, Q., Gao, L., Liu, J. (2023). Effect of vibration on performance of pneumatic rapeseed precision metering device (振动对气力式油菜精量排种器性能影响). *Journal of Huazhong Agricultural University*, Vol.42, No.2, pp.233-242. Wuhan/China.